ECS Transactions, 57 (1) 255-267 (2013)
10.1149/05701.0255ecst ©The Electrochemical Society

Power-to-Storage – The Use of an Anode-Supported Solid Oxide Fuel Cell as a High-Temperature Battery

Norbert H. Menzler, Andreas Hospach, Leszek Niewolak, Martin Bram, Oleg Tokariev, Cornelius Berger, Peter Orzessek, Willem J. Quadakkers, Qingping Fang and Hans Peter Buchkremer

Forschungszentrum Jülich Institute of Energy and Climate Research - IEK
52425 Jülich, GERMANY

A novel high-temperature energy storage system based on an SOFC is presented (Power-to-Storage). The energy is stored as a metal/metal oxide which is part of the fuel side. However, in contrast to a classical SOFC, the fuel side is kept under stagnant hydrogen/water vapor. By using the cell as an electrolyzer (SOEC), the surplus electricity (from renewable energy sources) is used to charge the system by reducing a metal oxide. Vice versa, if energy is needed the system works as an SOFC thereby oxidizing the metal (discharging the battery). First results from storage material development and stack testing are presented.

Introduction

In 2010, the German government decided (1) that electricity production in Germany was to be completely transformed in the next 40 years. The goals arising from that decision are firstly that 80% of electricity should be generated from renewable energy sources such as wind, solar, geothermal energy and, secondly, that anthropogenic carbon dioxide emissions should be cut to 20% compared to 1990. Moreover, in 2011the government also decided to shut down the last nuclear power plant in 2022 (2). If these goals are to be reached the future energy supply will be dominated by volatile energy converters. However, in contrast the basic energy demand will not change compared to today. Thus there is an urgent need for energy storage during times of electricity surplus and for a reliable energy supply during times with high energy demand but no availability of wind or solar energy.

Various possibilities already exist for storing such surplus electricity such as pump accumulators, generation of hydrogen by electrolysis (low and high temperature; “Power-to-Fuel”; “Power-to-Gas”) or generation of methane by methanation of hydrogen, and storage in low-temperature batteries. The main disadvantage of hydrogen production is the storage of H_2, which needs either leak-proof hydrogen-impermeable canisters or which can be stored in inorganic media such as MgH_2 although these media have a relatively low storage capacity. The main advantage of hydrogen methanation is that a large storage capacity is already available in the natural gas pipelines and subsurface geological caverns. The major disadvantage compared to the production of pure hydrogen is the reduction in efficiency. With respect to low-temperature batteries, no batteries for the storage of large quantities of electricity are yet available and the storage capacity is limited even if state-of-the-art lithium ion batteries are used.

A novel type of high-temperature battery was first patented by Westinghouse in 1996 (3). Here the inventors described a high-temperature system which works by switching between electrolyzer and fuel cell mode and thus storing energy by reducing and oxidizing a material. However, in this patent only the basic principle of the system is described. The reduction and oxidation is performed by changing the oxygen partial pressure in a water vapor/hydrogen system. The material to be reduced and oxidized is iron. In 2011, Siemens published another patent (4) concerning the same type of battery but referring to various possible materials for the redox cycling (e.g. Ti, Zr, Co, Cr, Mn, Fe, Ni, Cu). In a third patent (5), Siemens published details of a stack which contains a "classical" SOFC and on the fuel side a stagnant atmosphere system based on H_2O/H_2. First publications concerning this type of high-temperature battery show the basic operating principle (6) and first results from stack tests (7) However, Siemens has now discontinued its R&D on high-temperature electrochemistry.

Forschungszentrum Jülich started its own work on this type of battery in 2011. Based on the well-known anode-supported solid oxide fuel cell system (8, 9), the main focus is placed on the development of storage materials.

Operational Principle

In Figure 1, the basic principle of operating the Power-to-Storage battery is explained.

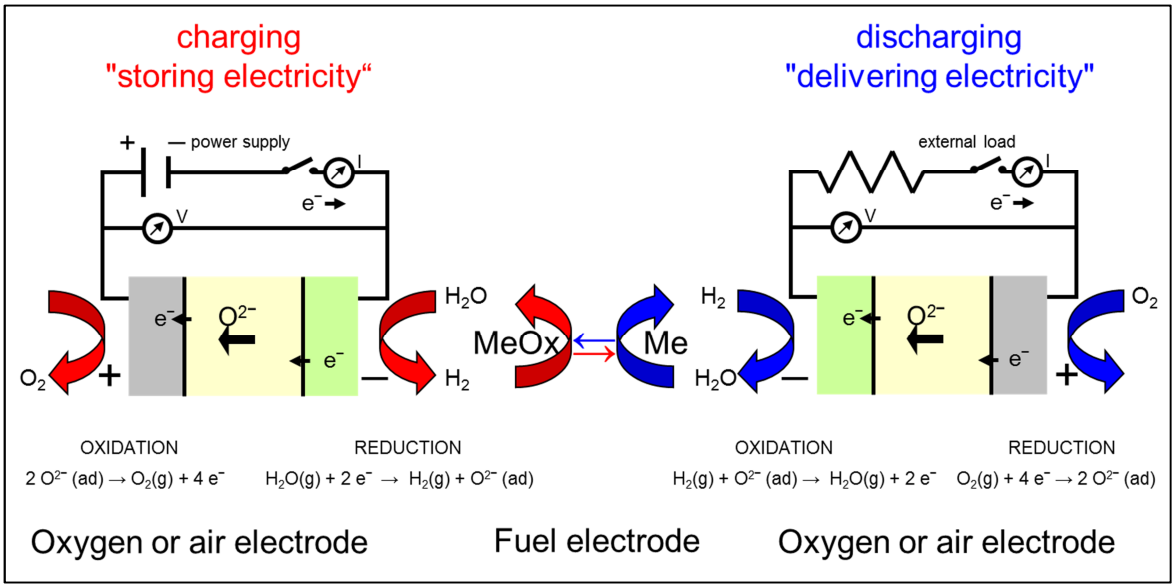

Figure 1. Basic operating principle of the high-temperature battery using an SOFC/SOEC (after Bert de Haart, IEK-9, Jülich)

During charging of the battery, the surplus electricity is used to operate the cell in electrolysis mode, thus generating hydrogen at the fuel side. The enhancement of the hydrogen partial pressure reduces the oxygen partial pressure and therefore the metal oxide is reduced. After finally reducing the complete metal oxide, the battery is in the

"completely charged state". If there is a higher demand for electricity than renewables can deliver, the battery operates in fuel cell mode by producing water vapor on the fuel side. Consequently, the oxygen partial pressure rises and oxidizes the metal. If the metal is in a fully oxidized state the battery is "empty". The main advantages of such a system are:

- Usage of only one electrochemical component (the cell) in both modes (fuel cell and electrolysis)
- Use of a cheap and widely available storage material (iron)
- On the fuel side no stream is necessary; only stagnant water vapor/hydrogen
- Air side operates with ambient air
- Less balance-of-plant necessary (e.g. no reformer, afterburner) than in conventional SOFC systems
- High efficiency of the well-known SOFC systems
- Modularity; such systems can be built up on a small scale in houses, on a medium scale in containers, e.g. for residential blocks or industries, or on a large scale near the coast to bridge electricity generation by off-shore wind power and electricity demand on shore

The Operation Window

In order to develop a storage material for the high-temperature battery, the basic requirement is the operation window, which means the parameters at which such a system has to be operated. This includes parameters such as temperature, lifetime, fuel mixture, current density, galvanostatic or potentiostatic operation potentiostatically. The two main parameters for storage are the operating temperature and the oxygen partial pressures for reduction and oxidation. The operating temperature was set at 700-800°C. There is an upper and a lower limit for the oxygen partial pressure. The upper limit is the oxidation potential of the nickel phase within the substrate and the anode of the fuel cell. This partial pressure is 800°C ~ 10^{-14} bar (see Figure 2). The lower limit is given by the oxygen partial pressure which is set by the water vapor / hydrogen ratio; this pressure is temperature-dependent, and at 800°C and a mixture of 80% H_2O and 20% H_2 it is ~ $10^{-19.5}$ bar (see Figure 3). Comparing these two limits minimizes the choice of materials which can be reduced and oxidized. Possible pure candidates are: cobalt, tungsten, molybdenum, iron, tin and cadmium. Sn is in a liquid state at the envisaged operating temperature, and Cd and Co are relatively toxic, Mo and W display high vapor pressure at these temperatures and atmospheric conditions, and thus iron seems to be the best material choice with respect to toxicity, physical and chemical parameters, availability and costs.

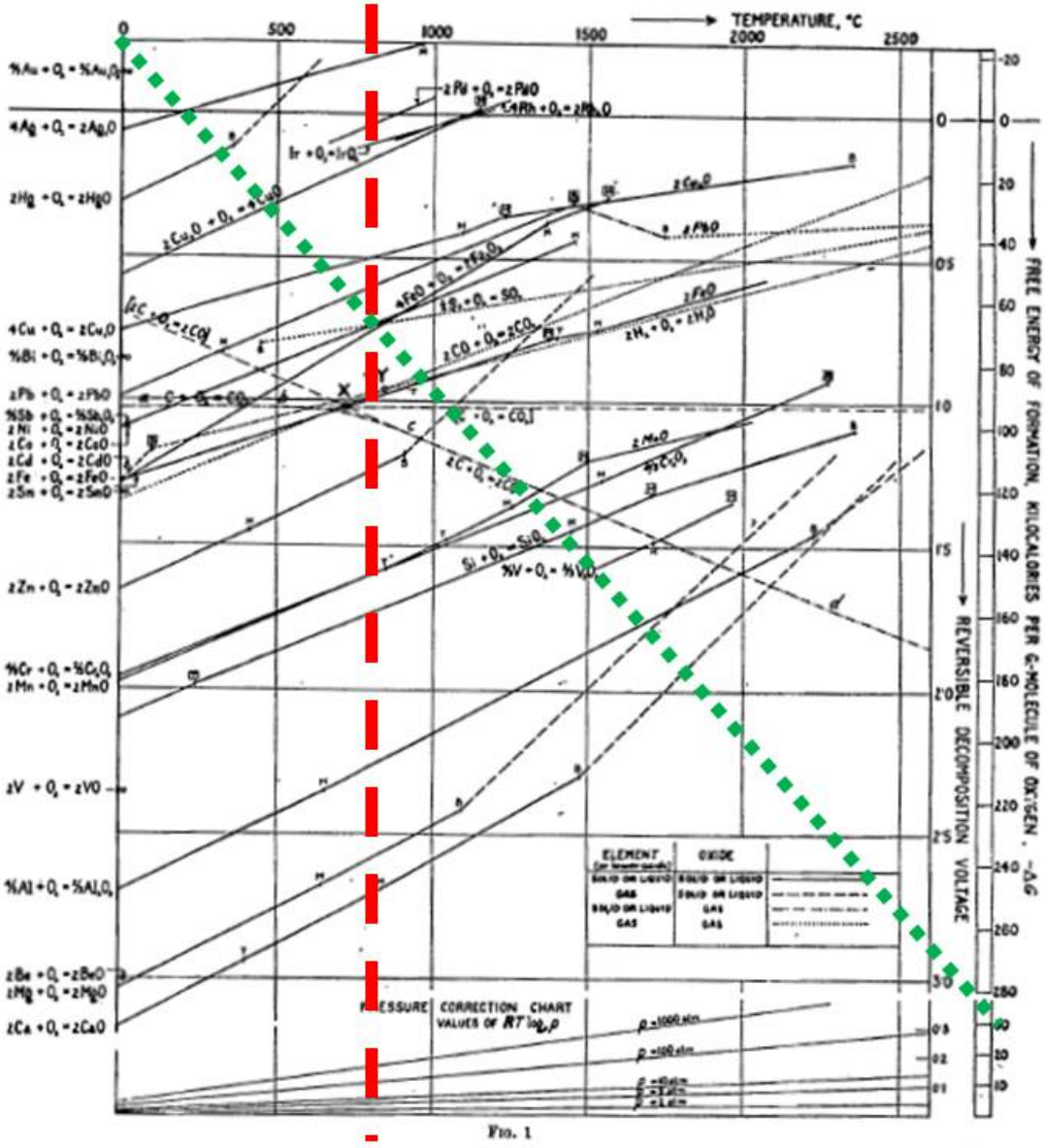

Figure 2. Ellingham diagram. The dashed line represents the operating temperature of the system (800°C) and the dotted line represents the line for the reaction 2 Ni + $O_2 \rightarrow$ 2 NiO [modified after (11)]

Development of Storage Material

Pure Iron

The first possibility of developing a storage material based on iron is the use of pure iron oxide as the starting material. The reason for choosing iron oxide is simple: all ceramic-related manufacturing techniques can be adapted and all sintering can be done in air and thus the fabrication of the storage structure is easy and cheap. Therefore the first samples were prepared by pressing small disks 15 mm in diameter and 3-5 mm in thickness. These pellets were subsequently redox cycled on a tubular furnace with an

alumina tube and placed on alumina supports. The redox conditions were: 800°C and the atmosphere alternated between Ar / 2% H_2 as the reducing gas and Ar / 2% H_2 / 7% H_2O as the oxidizing gas. After several redox cycles, the samples were removed and characterized by optical, confocal and scanning electron microscopy to identify the microstructure and by X-ray diffraction to examine the crystal structure and to calculate the amounts of phases formed. Furthermore, for all pellet and bar tests one cycle represents one atmosphere. That is to say, two cycles mean one oxidizing and one reducing step. The minimum number of cycles was 10 / 11 (10 cycles oxidized state, 11 cycles reduced state). Figure 4 shows cross sections of a pure iron oxide sample cycled 11 times.

Two findings can be clearly seen from Fig. 4. First, the microstructure seems to be relatively dense and thus diffusion paths for the hydrogen and the water vapor become long, and second, an outer rim is formed on the pellet. This rim is composed of a dense layer about 100µm in thickness. The layer also displays a double structure: the outside is reduced iron while the inner part is iron oxide. Due to the fact that this sample should be in a reduced state, the micrograph shows that the rim formation prevents the ongoing reduction of iron and thus drastically limits the storage capacity of the material. This finding implies that rim formation and densification must be suppressed.

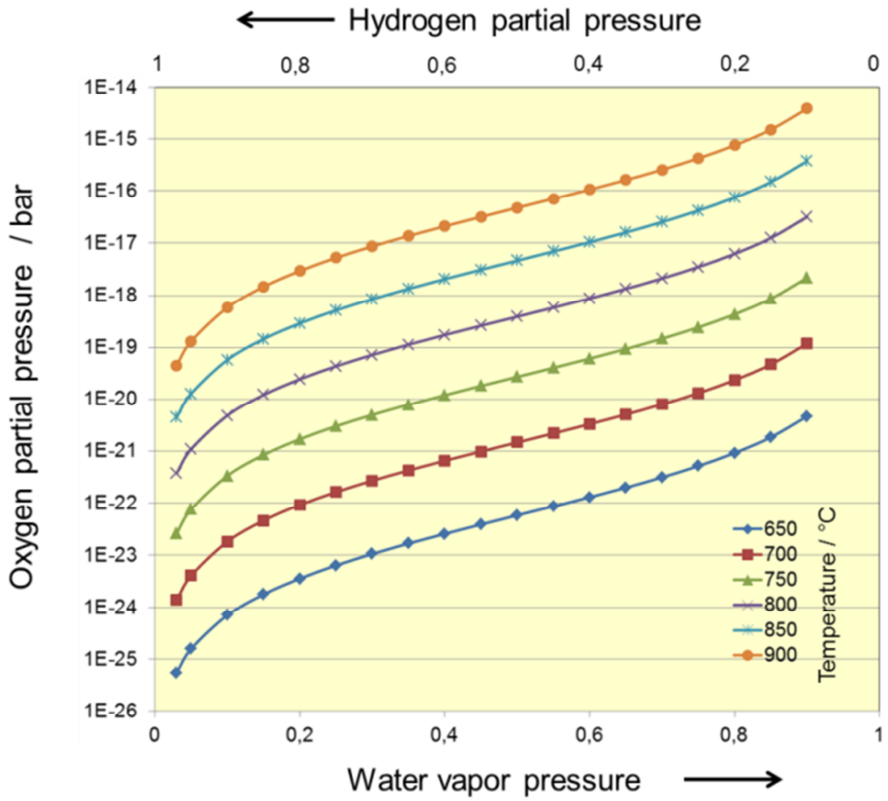

Figure 3. Dependence of the resulting oxygen partial pressure on the ratio of water vapor pressure to hydrogen vapor pressure (courtesy B. de Haart, IEK-9, Forschungszentrum Jülich)

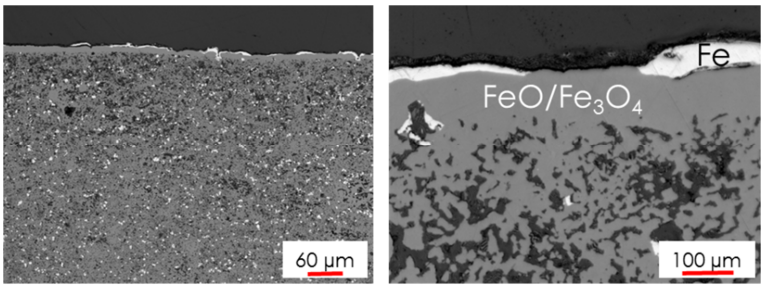

Figure 4. Confocal microscopy micrographs of a pure iron / iron oxide storage material after 11 redox cycles (now in reduced state); left: overview, right: higher magnification of upper side of pellet

Iron With Oxide Skeleton

To minimize the tendency to agglomerate (due to the high sintering activity of metallic iron at 800°C) and to suppress the outer rim formation, a second material acting as a backbone skeleton and thus minimizing the sintering of iron was introduced. The first choice of material was yttria-stabilized zirconia (8YSZ), because in the SOFC the anode is composed in a similar way (Ni + 8YSZ).

Both powders were mechanically mixed and pressed in the same way as the pure iron pellet (ratio: 70 vol% Fe_2O_3, 30 vol% 8YSZ). The high amount of iron in the oxide mixture should retain its capacity because the zirconia acts as an inert material (with respect to the redox cycling). By doing so, the microstructure becomes more porous. However, as can be seen from Fig. 5, the iron still tends to agglomerate and form an outer rim.

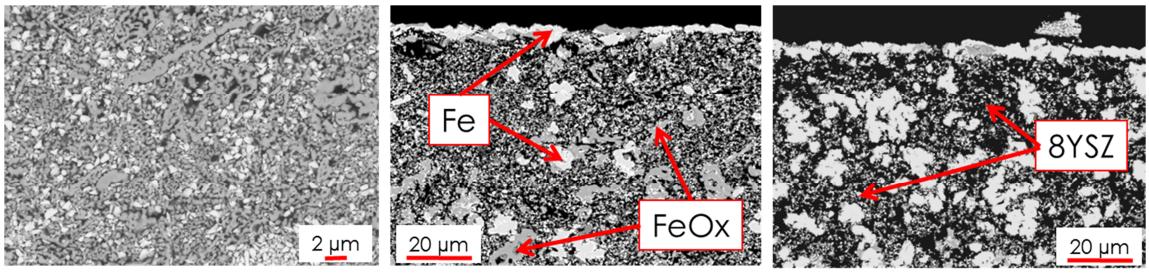

Figure 5. SEM cross sections of iron oxide / 8YSZ storage material after processing and after 11 redox cycles (reduced state); left: original state after pressing and sintering at 900°C; middle and right: after 11 cycles

In Fig. 5, it can be clearly seen that the iron has again agglomerated even in the inner part of the pellet and that also an outer rim has formed. Again rim formation prevents the complete reduction of iron, as proven by EDX point analysis which shows iron oxide phases.

Changing the supplier of the 8YSZ material (from Tosoh Corp., Japan, to UCM, Germany), introducing a pore former (graphite) or varying the pressing parameters do not basically affect the agglomeration and rim formation. The only influence is that rim

formation seems to be delayed, which means that after the same number of redox cycles the rim is less thick, pronounced and dense (more island-like).

In the next attempt, the ratio of Fe_2O_3 / 8YSZ was changed from 70: 30 vol.% to 30 : 70 vol.%. Figure 6 shows the microscopic results after 11 cycles.

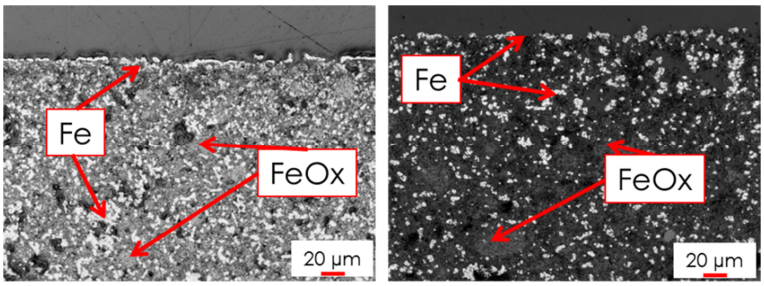

Figure 6. Confocal microscopy micrographs of an iron / 8YSZ (30 / 70 vol.%) storage material after left 10 (oxidized) and right 11 (reduced) redox cycles

It is obvious from Fig. 6 that both rim formation and agglomeration are less pronounced and thus it can be concluded that a reduced amount of iron within the storage material is a possible way to maintain its activity. However, the reduced amount of iron also means less storage capacity. Table 1 lists the percentage of phases detected by X-ray after three different cycles.

TABLE I. Phases Formed after Redox Cycling of the Iron / 8YSZ Storage (30/70 vol.%)

State	Cycles	Fe [%]	FeO [%]	Fe_3O_4 [%]	8YSZ [%]	ZrO_2 [%]
After sintering	--		30		70	
Oxidized	10	--	20	10	65	5
Reduced	11	30	--	--	65	5
Reduced	41	30	--	--	60	10

The following can be concluded from Table 1:

- The 8YSZ decomposes partly and monoclinic zirconia is formed
- In the oxidized state the iron exists in two phases, i.e. iron monoxide (wüstite) and di-iron tri-oxide (magnetite)
- Enhanced redox cycling reduces the amount of stabilized zirconia and, vice versa, increases the amount of pure zirconia

The reason for the outward diffusion of iron and subsequent rim formation might be that during oxidation the amount of p_{O2} in the surrounding phase is higher than in the storage material. Thus iron first oxidizes on the outer surface of the material. Ongoing oxidation occurs by diffusion of iron ions through the oxide layer formed because the diffusion coefficient of iron in iron oxide is higher than that of oxygen. Therefore, during oxidation, continuous material transport takes place from the inside of the storage

material to the outside (in summary, the complete iron "moves" towards the higher p_{O2}). During the next cycling step –reduction – no such driving force for the iron exists and it thus forms a layer on the outside which agglomerates due to its high sintering activity. As a consequence, more and more of the initial single iron islands are from (during every redox cycle) and constitute a continuous layer which becomes thicker and thicker with cycling time (however, this hypothesis is still not proven).

Finally, other oxides have been tested as a secondary skeleton phase (70 vol.% iron oxide). Partially stabilized zirconia, yttria, strontium oxide, alumina, and silica can be mentioned here. In all cases, neither of the effects, i.e. iron agglomeration and rim formation, can be suppressed. Therefore such storage material has to be stabilized by i) a low amount of functional oxide or by ii) the formation of intermediate double oxide phases which can form in a reducing environment with iron and a second pure oxide (see next section).

Iron with Second Oxide for Intermediate Oxide Formation

The idea behind this configuration is that it might be possible to suppress iron agglomeration and outward diffusion by using a double or triple oxide containing iron and a second metal which forms and remains stable under the oxidizing conditions present during cycling and which decomposes during reduction into metallic iron and the second metal oxide. The basic reaction (1.1) should be as follows:

$$Fe_xB_yO_z \rightarrow \text{reduction} \rightarrow Fe + B_yO_w \rightarrow \text{oxidation} \rightarrow Fe_xB_yO_z \qquad (1.1)$$

A prerequisite for such a reaction mechanism is that two oxides exist which are stable depending on oxygen partial pressure at the operating temperatures (700-800°C). Additionally, the stability / non-stability is limited to the p_{O2} between $10^{-19.5}$ and 10^{-14} bar. Only a limited number of oxide phases are capable of fulfilling these requirements. Possible candidates are oxides of iron with calcium oxide, titania, ceria, chromia, magnesia, manganese or copper.
The following procedures for the individual oxide pairs have been proven to be the same as described for pure iron and iron with skeleton oxide.

$Fe_2O_3 + CaO + ZrO_2$	formation of $CaZrO_3$ which acts as an inert skeleton (same as with 8YSZ)
$Fe_2O_3 + TiO_2 + ZrO_2$	formation of $TiFe_2O_5$ which cannot be re-reduced and thus iron is not available for the ongoing storage reaction
$Fe_2O_3 + CeO_2$	formation of $CeFeO_3$ which cannot be re-reduced
$Fe_2O_3 + Cr_2O_3$	formation of $FeCr_2O_4$ which cannot be re-reduced
$Fe_2O_3 + TiO_2$	formation of $FeTi_2O_4$ which cannot be re-reduced
$Fe_2O_3 + Mn_2O_3$	after sintering: 55% Fe_2O_3, 30% Mn_3O_4, 15% $MnFe_2O_4$ after oxidation (cycle 10): 25% FeO, 5% Fe_3O_4, 70% $MnFeO_2$ after reduction (cycle 41): 20% Fe, 10% FeO, 70% $MnFeO_2$ low amount of reactive iron

Fe_2O_3 + MgO	after sintering: 30% Fe_2O_3, 10% MgO, 60% $MgFe_2O_4$ after oxidation (cycle 10): 30% FeO, 50% $MgFeO_2$, 20% $MgFe_2O_4$ after reduction (cycle 11): 30% Fe, 10% FeO, 60% $MgFeO_2$ after reduction (cycle 41): 20% Fe, 20% FeO, 60% $MgFeO_2$ the more redox cycles the less iron is reactive
Fe_2O_3 + CuO	after sintering: 20% Fe_2O_3, 25% CuO, 55% $CuFe_2O_4$ (tetragonal) after oxidation (cycle 40): 20% FeO, 25% Cu, 55% $CuFe_2O_4$ (cubic) after reduction (cycle 41): 25% Fe, 20% FeO, 40% Cu, 15% $CuFe_2O_4$ outer rim formation consisting of Fe, iron oxide and iron-copper oxide; thus same behavior as with inert skeleton
Fe_2O_3 + CaO	after sintering: 15% Fe_2O_3, 5% CaO, 80% $CaFe_2O_4$ after oxidation (cycle 10): 20% $Ca_2Fe_2O_5$, 80% $CaFe_3O_5$ after reduction (cycle 11): 30% Fe, 50% $Ca_2Fe_2O_5$, 20% $CaFe_3O$ after reduction (cycle 41): 35% Fe, 65% $Ca_2Fe_2O_5$ amount of reactive iron increases with redox cycles (system not previously in equilibrium); $\Rightarrow$ promising material combination

Based on the above-mentioned material combinations, the only oxide with long-term stability which can be easily oxidized and reduced within the envisaged operational window is the combination of iron oxide and calcium oxide. These types of pellets were produced by using not calcium oxide but rather calcium carbonate. During sintering the carbonate decomposes and forms the mixed oxide and volatile carbon dioxide. Due to the gas formation, additional porosity is introduced and offers the possibility of producing a storage material with a highly reactive surface and thus high capacity and quick reactivity.

Stack Testing

Parallel to the development of the storage material, the first stack tests were performed. A standard Jülich anode-supported SOFC was used (type A) as the core component (8). The Jülich F10 design was chosen as the stack type (cell size 100 x 100mm²; No.: F 1002-148) (9). In contrast to the classical SOFC stack, on the fuel side channels were mechanically cut crosswise to the normal gas flow direction. Storage material composed of 70 vol.% Fe_2O_3 and 30 vol.% 8YSZ, prepared by tape casting according to (10) and sintering at 900°C, was placed in these 9 channels (geometry: ~ 90 x 6 x 1 mm³) during stack assembly. The stack was sealed and the NiO was reduced according to our internal standard procedure. After measurement of SOFC performance, the stagnant atmosphere on the fuel side was realized by steam with a gauge pressure of about 10 hPa. Assuming a constant charging and discharging rate, the current density can be adjusted according to the expected charging and discharging time. Based on this calculation, a current density of 250 mA/cm² and a charging time of 40 min were chosen for the first test. As shown in period 4 in Fig. 7, the cell voltages increased rapidly at 250 mA/cm². By decreasing the current density down to 150 mA/cm², two plateaus in cell voltages can be clearly seen during charging and discharging. Those two plateaus correspond well to the equilibrium between Fe/FeO and Fe/Fe_2O_3, which was confirmed by the OCVs (open cell voltage; 970 mV and 900 mV at 800°C, respectively) during

charging and discharging. With 150 mA/cm², a maximum charging time of 58 min was reached, which corresponds to ~70% of the theoretical time assuming that the charging rate is constant throughout the complete charging process. After evaluating both stack performance and functionality of the test bench under ROB mode in manual operation, the stack was operated automatically (automatic switching between charging and discharging) with the same charging and discharging time of 35 min. Based on the previous test results, a maximum charging time (under 150 mA/cm²) of 58 min was taken before automatic operation, so that the storage material started in a more reduced state. It was found that both charging (FeO reduction) and discharging (Fe oxidation) voltages decreased continually after each charging/discharging cycle, which indicated that the oxidation process could be easier than the reduction process despite the same amount of charge being transferred during the same charging and discharging time. Also some internal leakage may have influenced this behavior. Based on these results, a charging time of 2000 s and a discharging time of 1800 s were chosen for the automatic ROB operation as shown in Fig. 8. Since there would be always more Fe reduced after each cycle due to the longer charging (reduction) time, automatic operation was started with a more oxidized state of the storage material. Under these conditions, the stack was operated stably in ROB mode for nearly 320 cycles. It was decided not to continue further cycling to investigate the storage material.

I-V curves and calculated ASRs at 0.4 A/cm² before and after nearly 320 ROB cycles are shown in Fig. 9. The stack still behaved quite well, although a ~20% rise in ASR can clearly be seen. The fast voltage drop at high current densities in fuel cell mode could be an indication of possible electrode degradation after ROB operation, which needs to be investigated further.

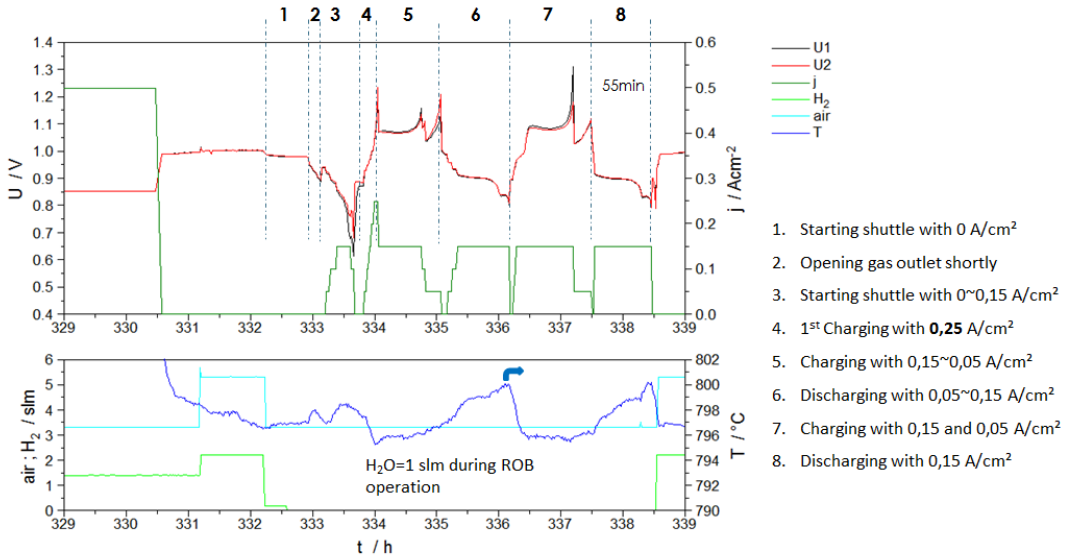

Figure 7. Time plot redox cycle stack F 1002-148 (current density always with positive scale)

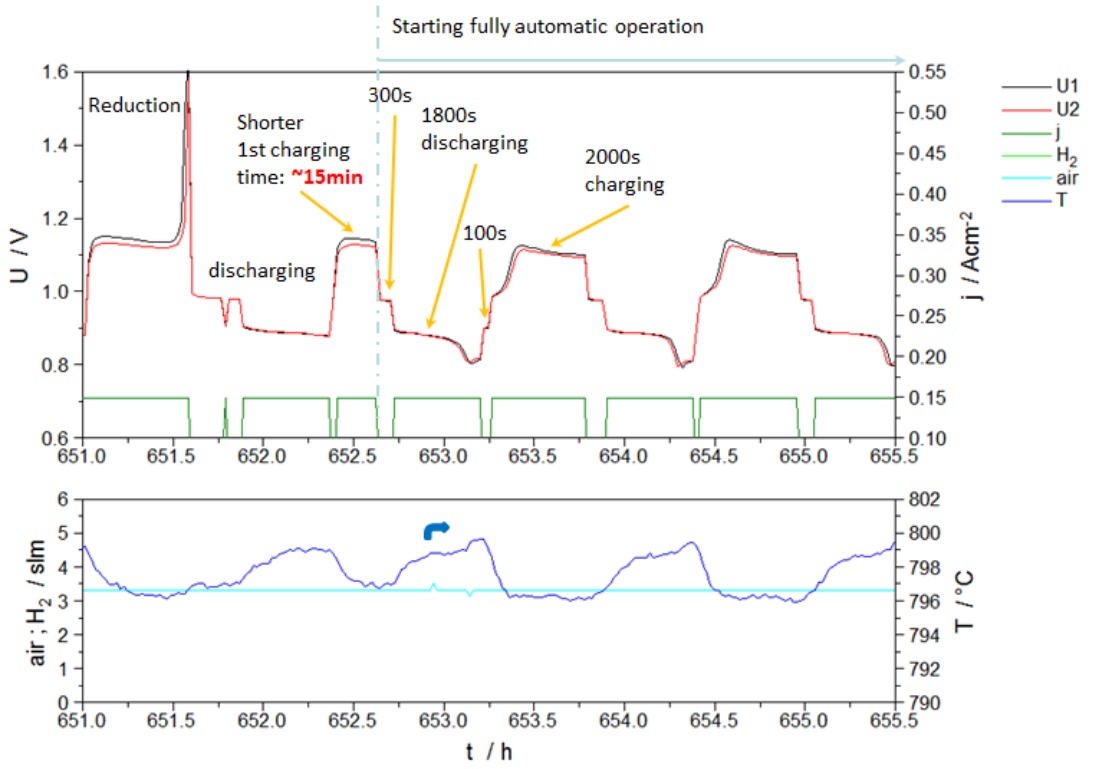

Figure 8. Stack F 1002-148 - Starting automatic ROB operation with different charging and discharging times (current density always with positive scale)

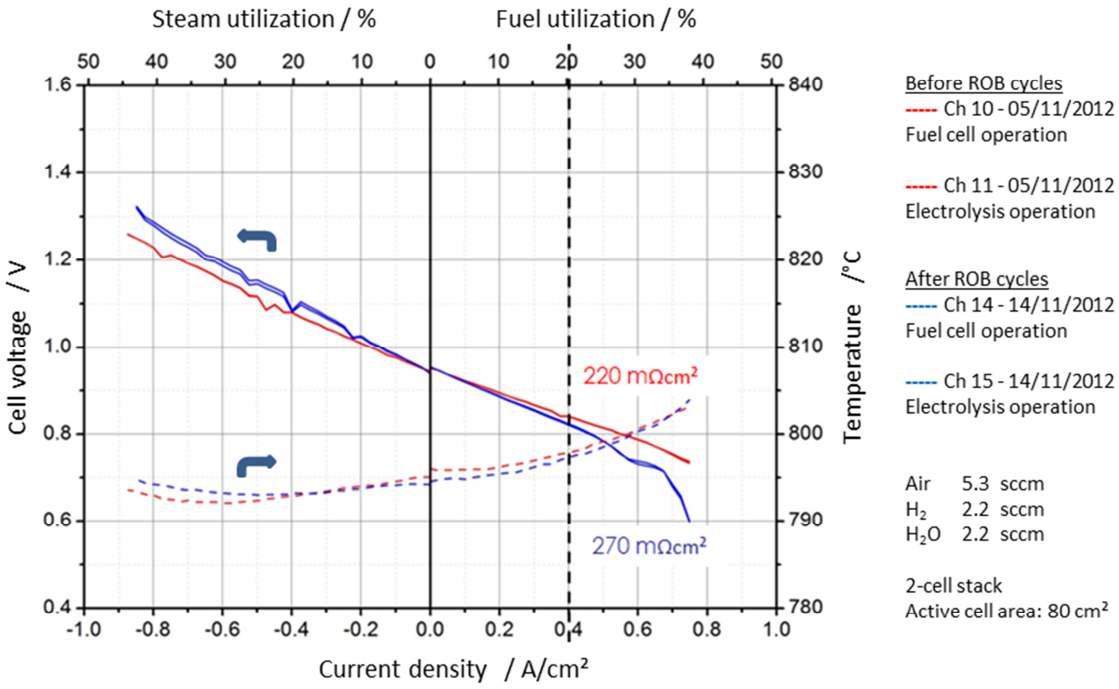

Figure 9. I-V-curve of both cells in both modes of stack F 1002-148

A post-test analysis is always performed after each stack shutdown. This examination is still in progress.

Conclusions

As part of a project funded by the German government, a novel type of high-temperature battery is being developed. The basic components are a classical solid oxide fuel cell stack based on anode-supported SOFCs. The main difference is that the fuel side is operated under a stagnant water vapor / hydrogen mixture to reduce and oxidize a metallic storage material. The metal used was iron due to its wide availability, costs and ideal physical and chemical parameters with respect to the chosen operating conditions. The operating temperature was 800°C and the oxygen partial pressure at the fuel side varied between $10^{-19.5}$ (reducing) and 10^{-14} (oxidizing) bar. First furnace tests of pressed storage pellets show that a storage material based on single iron oxide or iron oxide with an inert skeleton of a second oxide is formed during redox cycling and that iron agglomerates and an outer iron rim results which hinders or minimizes ongoing oxidation / reduction. Both effects can be suppressed by adding a reactive second oxide which under higher p_{O2} forms a double oxide and under reducing conditions metallic iron and a second oxide. A first stack test with a storage material based on Fe_2O_3 and 8YSZ was successfully tested for 320 redox cycles. Post-test analysis of that stack is in progress. The stack test proves the basic functionality of the SOFC stack operated in fuel cell and electrolysis mode, termed Power-to-Storage.

Future work will focus on the development of a better (higher capacity, quicker reaction) storage material (including microstructural optimization, material selection), the basic electrochemical characterization of the cells in swinging mode (including storage), stack testing (including learning how to operate such stacks) and intensive post-test analysis for further developments.

Acknowledgements

The authors gratefully acknowledge support from the SOFC group at Forschungszentrum Jülich, including all steps of development, manufacturing, stacking and testing. Additionally the German Federal Ministry of Education and Research (BMBF) is acknowledged for funding the MeMO project under contract No. 03EK3017 (July 2012 – June 2015).

References

1. http://www.bundesregierung.de/Content/DE/_Anlagen/2012/02/energiekonzept-final.pdf?__blob=publicationFile&v=5
2. http://www.bmu.de/service/publikationen/downloads/details/artikel/dreizehntes-gesetz-zur-aenderung-des-atomgesetzes/?tx_ttnews[backPid]=1091
3. WO 96/23322 International Patent Application, 01.08.1996
4. US 2011/0033769 A1 US Patent Application Publication, 02.10.2011
5. US 2012/0328972 A1 US Patent Application Publication, 27.12.2012
6. Xu N., Li X., Zhao X., Goodenough J.B. and Huang K.: A novel solid oxide redox flow battery for grid energy storage. Energy Environ. Sci. **4**, 4942 (2011).

7. Drenckhahn W., Kühne M., Soller T., Litzinger K., Shull J., Lu C., Greiner H., Landes H., Leonide A. and Schuh C.: A novel high temperature metal – air battery. Proc. 222nd ECS Meeting, 07-12.10.2012, Honolulu, USA, Session B1, 465-476
8. Han F., Mücke R., van Gestel T., Leonide A., Menzler N.H., Buchkremer H.P. and Stöver D.: Novel high-performance solid oxide fuel cells with bulk ionic conductance dominated thin-film electrolytes. *J. Power Sources*, **218**, 157 (2012).
9. Blum L., de Haart L.G.J., Malzbender J., Menzler N.H., Remmel J. and Steinberger-Wilckens R.: Recent results in Jülich solid oxide fuel cell technology developments. *J. Power Sources*, **241**, 477 (2013)
10. Schafbauer W., Menzler N.H. and Buchkremer H.P.: Tape casting of anode supports for solid oxide fuel cells at Forschungszentrum Jülich. Int. J. Appl. Ceram. Technol. Available online 4 OCT 2012, DOI: 10.1111/j.1744-7402.2012.02839.x
11. http://onlinelibrary.wiley.com/doi/10.1002/jctb.5000630501/pdf. Copied and modified from original article: Ellingham H.J.T.: Reducibility of oxides and sulphides in metallurgical processes. *J. Society Chemical Industry*, **63** (5), 125, (1944)